

# Post-collapse dynamics of self-gravitating Brownian particles in $D$ dimensions

Clément Sire and Pierre-Henri Chavanis

May 22, 2019

Laboratoire de Physique Théorique (FRE 2603 du CNRS), Université Paul Sabatier,  
 118, route de Narbonne, 31062 Toulouse Cedex 4, France  
 E-mail: *Clement.Sire@irsamc.ups-tlse.fr* & *Chavanis@irsamc.ups-tlse.fr*

## Abstract

We address the post-collapse dynamics of a self-gravitating gas of Brownian particles in  $D$  dimensions, in both canonical and microcanonical ensembles. In the canonical ensemble, the post-collapse evolution is marked by the formation of a Dirac peak with increasing mass. The density profile outside the peak evolves self-similarly with decreasing central density and increasing core radius. In the microcanonical ensemble, the post-collapse regime is marked by the formation of a “binary”-like structure surrounded by an almost uniform halo with high temperature. These results are consistent with thermodynamical predictions.

## 1 Introduction

In a recent series of papers [1, 2, 3], we have studied the dynamics and thermodynamics of self-gravitating Brownian particles confined within a spherical box of radius  $R$  in a space of dimension  $D$ . The particles are subject to self-gravity, to a friction originated from the presence of an inert gas and to a stochastic force (modeling turbulent fluctuations, collisions,...). For simplicity, we have considered the strong friction limit and reduced the problem to the study of the Smoluchowski-Poisson system. This model is interesting to develop because it displays the same qualitative properties (phase transitions, collapse, finite time singularity,...) as more realistic gravitational models [4, 5, 6, 7, 8] and is easier to study in a first step. It could find astrophysical applications in the process of planet formation in the solar nebula where a friction with the gas is present (see, e.g., [9]). It can also provide a simplified model for the violent relaxation of collisionless stellar systems [10]. Coincidentally, this model also appears in biology to model the chemotactic aggregation of bacterial populations [13]. Rigorous results concerning the existence and unicity of solutions have been established by mathematicians (we refer to [11, 12] for a connexion and for a detailed list of references).

In previous works, we focused on the pre-collapse regime. In the canonical situation (fixed temperature  $T$ ) we showed that a critical temperature  $T_c$  exists below which the system undergoes a gravitational collapse leading to a finite time singularity at  $t = t_{coll}$ . For  $t \rightarrow t_{coll}$ , the evolution is self-similar in the sense that the density profile evolves as  $\rho(r, t) = \rho_0(t)f(r/r_0(t))$  where  $f(x)$  is independent on time. For  $x \rightarrow +\infty$ ,  $f(x) \sim x^{-\alpha}$  with  $\alpha = 2$ . The central density

increases as  $\rho_0 \sim (t_{coll} - t)^{-1}$  and the core radius decreases as  $r_0 \sim (t_{coll} - t)^{1/\alpha}$ . For  $T = 0$ , the exponent is  $\alpha = 2D/(D+2)$ . In the microcanonical situation (where  $T(t)$  evolves in time so as to conserve energy), there exists a critical energy  $E_c$  (Antonov energy) below which the system collapses. For  $t \rightarrow t_{coll}$ , there exists a pseudo-scaling regime where  $\alpha$  passes very slowly from  $\alpha_{max} = 2.21\dots$  to  $\alpha = 2$ . Numerical simulations suggest that  $T(t)$  remains finite at  $t = t_{coll}$  so that the true scaling regime corresponds to  $\alpha = 2$ , as in the canonical situation [3, 14].

What happens after  $t_{coll}$ ? By investigating the case  $T = 0$ , we found in [2] that the evolution continues in the post-collapse regime with the formation of a Dirac peak accreting more and more mass as  $M(t) \sim (t - t_{coll})^{D/2}$  while the density outside the peak evolves self-similarly with decreasing central density  $\rho_0 \sim (t - t_{coll})^{-1}$  and increasing core radius  $r_0 \sim (t - t_{coll})^{\frac{D+2}{2D}}$ . Our aim in this paper is to investigate the post collapse regime for  $T \neq 0$  in both canonical and microcanonical ensembles. In Sec. 2, we set the notations and recall the main results concerning the pre-collapse dynamics. In Sec. 3, we study the post-collapse dynamics at  $T = 0$  by a method different from [2], which can be generalized at finite temperature. The post collapse dynamics at  $T > 0$  is precisely considered in Sec. 4. In the canonical ensemble, we show that the system forms a Dirac peak whose mass increases as  $M(t) \sim (t - t_{coll})^{D/2-1}$  while the density profile for  $r > 0$  expands self-similarly with  $\rho_0 \sim (t - t_{coll})^{-1}$  and  $r_0 \sim (t - t_{coll})^{1/2}$ . For large times, the system is made of a Dirac peak of mass  $\sim M$  surrounded by a light gas of Brownian particles (with negligible self-interaction). Due to thermal motion, complete collapse takes an infinite time (contrary to the case  $T = 0$ ). For  $t \rightarrow +\infty$ , the mass contained in the Dirac peak increases as  $1 - M(t)/M \sim \exp(-\lambda t)$  where  $\lambda$  is the fundamental eigenvalue of a quantum problem. For  $T \rightarrow 0$ , we find that  $\lambda = 1/4T + c_D/T^{1/3} + \dots$ . In the microcanonical ensemble, the post-collapse regime is very pathological. The system tends to create a “Dirac peak of  $0^+$  mass” surrounded by a uniform halo with infinite temperature. The central structure is reminiscent of a “binary star” containing a weak mass  $2m \ll M = Nm$  but a huge binding energy comparable to the potential energy of the whole cluster. Since our model is essentially mean-field, the physical formation of binaries is replaced by the type of structures mentioned above. The formation of a “Dirac peak” containing the whole mass in canonical ensemble and the formation of “binaries” in microcanonical ensemble are expected from thermodynamical considerations [15, 16, 17, 18, 19, 2]. These are the structures which provoke a divergence of free energy (at fixed mass and temperature) and entropy (at fixed mass and energy) respectively. All these analytical results are confirmed by numerical simulations of the Smoluchowski-Poisson system in Secs. 5 and 6. We were able in particular to “cross the singularity” at  $t = t_{coll}$  and describe the post-collapse dynamics.

## 2 Collapse dynamics of self-gravitating Brownian particles

### 2.1 The Smoluchowski-Poisson system

At a given temperature  $T$  controlling the diffusion coefficient, the particle density  $\rho$  satisfies the following coupled equations:

$$(1) \quad \frac{\partial \rho}{\partial t} = \nabla \left[ \frac{1}{\xi} (T \nabla \rho + \rho \nabla \Phi) \right],$$

$$(2) \quad \Delta \Phi = S_D G \rho,$$

where  $\Phi$  is the gravitational potential, and  $S_D$  is the surface of the unit  $D$ -dimensional sphere.

From now on, we set  $M = R = G = \xi = 1$  and we restrict ourselves to spherically symmetric solutions. The equations of the problem become

$$(3) \quad \frac{\partial \rho}{\partial t} = \nabla(T \nabla \rho + \rho \nabla \Phi),$$

$$(4) \quad \Delta \Phi = S_D \rho,$$

with proper boundary conditions in order to impose a vanishing particle flux on the surface of the confining sphere. These read

$$(5) \quad \frac{\partial \Phi}{\partial r}(0, t) = 0, \quad \Phi(1) = \frac{1}{2 - D}, \quad T \frac{\partial \rho}{\partial r}(1) + \rho(1) = 0,$$

for  $D > 2$ . For  $D = 2$ , we take  $\Phi(1) = 0$  on the boundary. Integrating Eq. (4) once, we can rewrite the Smoluchowski-Poisson system in the form of a single integrodifferential equation

$$(6) \quad \frac{\partial \rho}{\partial t} = \frac{1}{r^{D-1}} \frac{\partial}{\partial r} \left\{ r^{D-1} \left( T \frac{\partial \rho}{\partial r} + \frac{\rho}{r^{D-1}} \int_0^r \rho(r') S_D r'^{D-1} dr' \right) \right\}.$$

The total energy is given as the sum of the kinetic and potential contributions

$$(7) \quad E = \frac{D}{2} T + \frac{1}{2} \int \rho \Phi d^D \mathbf{r}.$$

The Smoluchowski-Poisson system is also equivalent to a single differential equation

$$(8) \quad \frac{\partial M}{\partial t} = T \left( \frac{\partial^2 M}{\partial r^2} - \frac{D-1}{r} \frac{\partial M}{\partial r} \right) + \frac{1}{r^{D-1}} M \frac{\partial M}{\partial r},$$

for the quantity

$$(9) \quad M(r, t) = \int_0^r \rho(r') S_D r'^{D-1} dr',$$

which represents the mass contained within the sphere of radius  $r$ . The appropriate boundary conditions are

$$(10) \quad M(0, t) = N_0(t), \quad M(1, t) = 1,$$

where  $N_0(t) = 0$ , except if the density develops a condensed Dirac peak contribution at  $r = 0$ , of total mass  $N_0(t)$ . It is also convenient to introduce the function  $s(r, t) = M(r, t)/r^D$  satisfying

$$(11) \quad \frac{\partial s}{\partial t} = T \left( \frac{\partial^2 s}{\partial r^2} + \frac{D+1}{r} \frac{\partial s}{\partial r} \right) + \left( r \frac{\partial s}{\partial r} + D s \right) s.$$

## 2.2 Self-similar solutions of the Smoluchowski-Poisson system

In [1, 2, 3], we have shown that in the canonical ensemble (fixed  $T$ ), the system undergoes gravitational collapse below a critical temperature  $T_c$  depending on the dimension of space. The density develops a scaling profile, and the central density grows and diverges at a finite time  $t_{coll}$ . The case  $D = 2$  was extensively studied in [2] and turns out to be very peculiar. Throughout this paper, we restrain ourselves to the more generic case  $D > 2$ , although other dimensions play a special role as far as static properties are concerned (see [2, 3]).

We look for self-similar solutions of the form

$$(12) \quad \rho(r, t) = \rho_0(t) f\left(\frac{r}{r_0(t)}\right), \quad r_0 = \left(\frac{T}{\rho_0}\right)^{1/2},$$

where the King's radius  $r_0$  defines the size of the dense core [20]. In terms of the mass profile, we have

$$(13) \quad M(r, t) = M_0(t) g\left(\frac{r}{r_0(t)}\right), \quad \text{with} \quad M_0(t) = \rho_0 r_0^D,$$

and

$$(14) \quad g(x) = S_D \int_0^x f(x') x'^{D-1} dx'.$$

In terms of the function  $s$ , we have

$$(15) \quad s(r, t) = \rho_0(t) S\left(\frac{r}{r_0(t)}\right), \quad \text{with} \quad S(x) = \frac{g(x)}{x^D}.$$

Substituting the *ansatz* (15) into Eq. (11), we find that

$$(16) \quad \frac{d\rho_0}{dt} S(x) - \frac{\rho_0}{r_0} \frac{dr_0}{dt} x S'(x) = \rho_0^2 \left( S''(x) + \frac{D+1}{x} S'(x) + x S(x) S'(x) + D S(x)^2 \right),$$

where we have set  $x = r/r_0$ . The variables of position and time separate provided that  $\rho_0^{-2} d\rho_0/dt$  is a constant that we arbitrarily set equal to 2. After time integration, this leads to

$$(17) \quad \rho_0(t) = \frac{1}{2} (t_{coll} - t)^{-1},$$

so that the central density becomes infinite in a finite time  $t_{coll}$ . The scaling equation now reads

$$(18) \quad 2S + xS' = S'' + \frac{D+1}{x} S' + S(xS' + DS).$$

The scaling solution of Eq. (18) was obtained analytically in [2] and reads

$$(19) \quad S(x) = \frac{4}{D-2+x^2},$$

which decays with an exponent  $\alpha = 2$ . This leads to

$$(20) \quad f(x) = \frac{4(D-2)}{S_D} \frac{x^2 + D}{(D-2+x^2)^2}, \quad g(x) = \frac{4x^D}{D-2+x^2}.$$

Note finally that within the core radius  $r_0$ , the total mass in fact vanishes as  $t \rightarrow t_{coll}$ . Indeed, from Eq. (13), we obtain

$$(21) \quad M(r_0(t), t) \sim \rho_0(t) r_0^D(t) \sim T^{D/2} (t_{coll} - t)^{D/2-1}.$$

Therefore, the collapse does not create a Dirac peak ("black hole").

In [2], we have also studied the collapse dynamics at  $T = 0$  for which we obtained

$$(22) \quad \rho_0(t) \sim S_D^{-1} (t_{coll} - t)^{-1},$$

as previously, but the core radius is not given anymore by the King's radius which vanishes for  $T = 0$ . Instead, we find

$$(23) \quad r_0 \sim \rho_0^{-1/\alpha},$$

with

$$(24) \quad \alpha = \frac{2D}{D+2}.$$

The scaling function  $S(x)$  is only known implicitly

$$(25) \quad \left[ \frac{2}{D+2} - S(x) \right]^{\frac{D}{D+2}} = K x^{\frac{2D}{D+2}} S(x),$$

where  $K$  is a known constant (see [2] for details),  $S(0) = \frac{2}{D+2}$ , and the large  $x$  asymptotics  $S(x) \sim f(x) \sim x^{-\alpha}$ . The mass within the core radius is now

$$(26) \quad M(r_0(t), t) \sim \rho_0(t) r_0^D(t) \sim (t_{coll} - t)^{D/2},$$

and it again tends to zero as  $t \rightarrow t_{coll}$ . Comparing Eq. (21) and Eq. (26) suggests that if the temperature is very small, an apparent scaling regime corresponding to the  $T = 0$  case will hold up to a cross-over time  $t_*$ , with

$$(27) \quad t_{coll} - t_* \sim T^{D/2}.$$

Above  $t_*$ , the  $T \neq 0$  scaling ultimately prevails.

### 3 Post-collapse dynamics at $T = 0$

So far, all studies concerning the collapse dynamics of self-gravitating Brownian particles have concentrated on the time period  $t \leq t_{coll}$ . A natural question arises: what is happening for  $t > t_{coll}$ ? The first possible scenario is that the state reached at  $t = t_{coll}$  is in fact a stationary state. However, it is easy to check (see [1]) that this is absolutely not the case.

The scenario that we are now exploring is the following. A central Dirac peak containing a mass  $N_0(t)$  emerges at  $t > t_{coll}$ , whereas the density for  $r > 0$  satisfies a scaling relation of the form

$$(28) \quad \rho(r, t) = \rho_0(t) f\left(\frac{r}{r_0(t)}\right),$$

where  $\rho_0(t)$  is now decreasing with time (starting from  $\rho_0(t = t_{coll}) \rightarrow +\infty$ ) and  $r_0(t)$  grows with time (starting from  $r_0(t = t_{coll}) = 0$ ). As time increases, the residual mass for  $r > 0$  is progressively swallowed by the dense core made of particles which have fallen on each other. It is the purpose of the rest of this paper to show that this scenario actually holds, as well as to obtain analytical and numerical results illustrating this final collapse stage.

In this section, we present an alternative treatment to that of [2], where this scenario was analytically shown to hold at  $T = 0$ . This new approach is a good introduction to the general  $T \neq 0$  case which is studied in the next section. We refer the reader to [2] for an explicit solution of the  $T = 0$  post-collapse regime, which we found, leads to a central peak containing all the mass in a finite time  $t_{end}$ .

For  $T = 0$ , the dynamical equation for the integrated mass  $M(r, t)$  reads

$$(29) \quad \frac{\partial M}{\partial t} = \frac{1}{r^{(D-1)}} M \frac{\partial M}{\partial r},$$

with boundary conditions

$$(30) \quad M(0, t) = N_0(t), \quad M(1, t) = 1.$$

We define  $\rho_0$  such that for small  $r$

$$(31) \quad M(r, t) - N_0(t) = \rho_0(t) \frac{r^D}{D} + \dots$$

Up to the geometrical factor  $S_D^{-1}$ ,  $\rho_0(t)$  is the central residual density (the residual density is defined as the density after the central peak has been subtracted). For  $r = 0$ , Eq. (29) leads to the evolution equation for  $N_0$

$$(32) \quad \frac{dN_0}{dt} = \rho_0 N_0.$$

As  $N_0(t) = 0$  for  $t \leq t_{coll}$ , and since this equation is a first order differential equation, it looks like  $N_0(t)$  should remain zero for  $t > t_{coll}$  as well. However, since  $\rho_0(t_{coll}) = +\infty$ , there is mathematically speaking no global solution for this equation and non zero values for  $N_0(t)$  can emerge from Eq. (32), as will soon become clear.

We then define

$$(33) \quad s(r, t) = \frac{M(r, t) - N_0(t)}{r^D},$$

which satisfies

$$(34) \quad \frac{\partial s}{\partial t} = \left( r \frac{\partial s}{\partial r} + Ds \right) s + \frac{N_0}{r^D} \left( r \frac{\partial s}{\partial r} + Ds - \rho_0 \right).$$

By definition, we have also  $s(0, t) = \rho_0(t)/D$ .

We now look for a scaling solution of the form

$$(35) \quad s(r, t) = \rho_0(t) S\left(\frac{r}{r_0(t)}\right),$$

with  $S(0) = D^{-1}$  and

$$(36) \quad \rho_0(t) = r_0(t)^{-\alpha},$$

where  $r_0$  is thus defined without ambiguity. Inserting this scaling *ansatz* in Eq. (34), and defining the scaling variable  $x = r/r_0$ , we find

$$(37) \quad \frac{1}{\alpha \rho_0^2} \frac{d\rho_0}{dt} (\alpha S + xS') = S(DS + xS') + \frac{N_0}{\rho_0 r_0^D} \frac{1}{x^D} (DS + xS' - 1).$$

Imposing scaling, we find that both time dependent coefficients appearing Eq. (37) should be in fact constant. We thus define a constant  $\mu$  such that

$$(38) \quad N_0 = \mu \rho_0 r_0^D,$$

and set

$$(39) \quad \frac{1}{\alpha \rho_0^2} \frac{d\rho_0}{dt} = -\kappa,$$

with  $\kappa > 0$ , as the central residual density is expected to decrease. Equation (39) implies that  $\rho_0 \sim (t - t_{coll})^{-1}$ , which along with Eq. (36) implies that  $N_0 \sim (t - t_{coll})^{D/\alpha-1}$ . We thus find a power law behavior for  $N_0$ , which in order to be compatible with Eq. (32), leads to

$$(40) \quad \rho_0(t) = \left( \frac{D}{\alpha} - 1 \right) (t - t_{coll})^{-1},$$

and then to

$$(41) \quad \kappa = \frac{1}{D - \alpha}.$$

We end up with the scaling equation

$$(42) \quad \frac{1}{D - \alpha} (\alpha S + xS') + S(DS + xS') + \mu x^{-D} (DS + xS' - 1) = 0.$$

From Eq. (42), we find that the large  $x$  asymptotics of  $S$  is  $S(x) \sim x^{-\alpha}$ . In a short finite time after  $t_{coll}$ , it is clear that the large distance behavior of the density profile ( $r \gg r_0$ ) cannot dramatically change. We deduce that the decay of  $S$  should match the behavior for time slightly less than  $t_{coll}$  for which  $S(x) \sim x^{-\frac{2D}{D+2}}$ . Hence the value of  $\alpha$  should remain unchanged before and after  $t_{coll}$ . Finally, we obtain the following exact behaviors for short time after  $t_{coll}$ :

$$(43) \quad \rho_0(t) = \frac{D}{2} (t - t_{coll})^{-1},$$

$$(44) \quad r_0(t) = \left( \frac{2}{D} \right)^{\frac{D+2}{2D}} (t - t_{coll})^{\frac{D+2}{2D}},$$

$$(45) \quad N_0(t) = \mu \left( \frac{2}{D} \right)^{\frac{D}{2}} (t - t_{coll})^{\frac{D}{2}}.$$

We note the remarkable result that the central residual density  $\rho(0, t) = S_D^{-1} \rho_0(t)$  displays a universal behavior just after  $t_{coll}$ , a result already obtained in [2]. Moreover, we find that  $N_0(t)$  has the same form as the mass found within a sphere of radius  $r_0(t)$  below  $t_{coll}$ , given in Eq. (26).

Moreover, the scaling function  $S$  satisfies

$$(46) \quad \frac{D+2}{D^2} \left( \frac{2D}{D+2} S + xS' \right) + S(DS + xS') + \mu x^{-D} (DS + xS' - 1) = 0.$$

The constant  $\mu$  is determined by imposing that the large  $r$  behavior of  $s(r, t)$  (or  $\rho(r, t)$ ) exactly matches (not simply proportional) that obtained below  $t_{coll}$ , which depends on the shape of the initial condition as shown in [2]. Equation (46) can be solved implicitly by looking for solutions of the form  $x^D = z[S(x)]$ . After cumbersome but straightforward calculations, we obtain the implicit form

$$(47) \quad 1 + \frac{x^D}{\mu} S(x) = \left[ 1 + \frac{x^D}{\mu} \left( S(x) + \frac{2}{D^2} \right) \right]^{\frac{D}{D+2}},$$

which coincides with the implicit solution given in [2]. Note that  $S(x)$  is a function of  $x^D$ . We check that the above result indeed leads to  $S(0) = D^{-1}$ , and to the large  $x$  asymptotics

$$(48) \quad S(x) \sim \mu^{\frac{2}{D+2}} \left( \frac{2}{D^2} \right)^{\frac{D}{D+2}} x^{-\frac{2D}{D+2}}.$$

Note finally that for  $T = 0$ ,  $N_0$  saturates to 1 in a finite time, corresponding to the deterministic collapse of the outer mass shell initially at  $r = 1$ . Indeed, using Gauss' theorem, the position of a particle initially at  $r(t=0) = 1$  satisfies

$$(49) \quad \frac{dr}{dt} = -r^{-(D-1)}.$$

The position of the outer shell is then

$$(50) \quad r(t) = (1 - Dt)^{1/D},$$

which vanishes for  $t_{end} = D^{-1}$ .

## 4 Post-collapse dynamics at $T > 0$

### 4.1 Scaling regime

In the more general case  $T \neq 0$ , we will proceed in a very similar way as in the previous section. We define again,

$$(51) \quad s(r, t) = \frac{M(r, t) - N_0(t)}{r^D},$$

where  $N_0$  still satisfies

$$(52) \quad \frac{dN_0}{dt} = \rho_0 N_0.$$

We now obtain

$$(53) \quad \frac{\partial s}{\partial t} = T \left( \frac{\partial^2 s}{\partial r^2} + \frac{D+1}{r} \frac{\partial s}{\partial r} \right) + \left( r \frac{\partial s}{\partial r} + Ds \right) s + \frac{N_0}{r^D} \left( r \frac{\partial s}{\partial r} + Ds - \rho_0 \right).$$

By definition, we have again  $s(0, t) = \rho_0(t)/D$ .

We look for a scaling solution of the form

$$(54) \quad s(r, t) = \rho_0(t) S \left( \frac{r}{r_0(t)} \right),$$

with  $S(0) = D^{-1}$ . As before, we define the King's radius by

$$(55) \quad r_0 = \left( \frac{T}{\rho_0} \right)^{1/2}.$$

For  $t < t_{coll}$ , we had  $s(r, t) \sim 4Tr^{-2}$  (or  $S(x) \sim 4x^{-2}$ ). In a very short time after  $t_{coll}$ , this property should be preserved, which implies that the post-collapse scaling function should also behave as

$$(56) \quad S(x) \sim 4x^{-2},$$

for large  $x$ . Inserting the scaling *ansatz* in Eq. (53), we obtain

$$(57) \quad \frac{1}{2\rho_0^2} \frac{d\rho_0}{dt} (2S + xS') = S'' + \frac{D+1}{x} S' + S(DS + xS') + \frac{N_0}{\rho_0 r_0^D} \frac{1}{x^D} (DS + xS' - 1).$$

Again, this equation should be time independent for scaling to hold, which implies that there exist two constants  $\mu$  and  $\kappa$  such that

$$(58) \quad N_0 = \mu \rho_0 r_0^D,$$

and

$$(59) \quad \frac{1}{2\rho_0^2} \frac{d\rho_0}{dt} = -\kappa,$$

with  $\kappa > 0$ , as the central residual density is again expected to decrease. Equation (59) implies that  $\rho_0 \sim (t - t_{coll})^{-1}$ , and then that  $N_0 \sim (t - t_{coll})^{D/2-1}$ . We thus find a power law behavior for  $N_0$ , which in order to be compatible with Eq. (52), leads to the universal behavior

$$(60) \quad \rho_0(t) = \left( \frac{D}{2} - 1 \right) (t - t_{coll})^{-1},$$

and then to

$$(61) \quad \kappa = \frac{1}{D-2}.$$

We end up with the scaling equation

$$(62) \quad \frac{1}{D-2} (2S + xS') + S'' + \frac{D+1}{x} S' + S(DS + xS') + \mu x^{-D} (DS + xS' - 1) = 0,$$

where  $\mu$  has to be chosen so that  $S(x)$  satisfies the condition of Eq. (56). Its value will be determined numerically in Sec. 5 for  $D = 3$ . Note that for small  $x$ , the pre-collapse scaling function satisfies  $S(x) - S(0) \sim x^2$ , whereas the post-collapse scaling function behaves as

$$(63) \quad S(x) - S(0) \sim x^D.$$

However, contrary to the  $T = 0$  case,  $S(x)$  is not purely a function of  $x^D$ .

Finally, we find that the weight of the central peak has a universal behavior for short time after  $t_{coll}$

$$(64) \quad N_0(t) = \mu \left( \frac{2}{D-2} \right)^{D/2-1} T^{D/2} (t - t_{coll})^{D/2-1}.$$

Note that  $N_0(t)$  behaves in a very similar manner to the mass within a sphere of radius  $r_0$  below  $t_{coll}$ , shown in Eq. (21). In addition, comparing Eq. (64) and Eq. (45), we can define again a post-collapse cross-over time between the  $T \neq 0$  and  $T = 0$  regimes

$$(65) \quad t_* - t_{coll} \sim T^{D/2},$$

which is similar to the definition of Eq. (27).

## 4.2 Large time limit

Contrary to the  $T = 0$  case, the complete collapse does not take place in a finite time as thermal fluctuations always allow for some particle to escape the central strongly attractive potential. In order to illustrate this point, and obtain more analytic insight on this matter, we will place ourselves in the extreme situation where almost all the mass has collapsed ( $N_0 \lesssim 1$ ), and only an infinitesimal amount remains in the residual profile.

In this limit, the residual density  $\rho(r, t)$  satisfies the Fokker-Planck equation

$$(66) \quad \frac{\partial \rho}{\partial t} = T \left( \frac{\partial^2 \rho}{\partial r^2} + \frac{D-1}{r} \frac{\partial \rho}{\partial r} \right) + \frac{1}{r^{D-1}} \frac{\partial \rho}{\partial r},$$

with boundary condition

$$(67) \quad T \frac{\partial \rho}{\partial r}(1, t) + \rho(1, t) = 0.$$

The problem indeed reduces to the study of a very light gas (*i.e.* with negligible self-interaction) of Brownian particles submitted to the gravitational force  $\mathbf{F} = -(GM/r^{D-1})\mathbf{e}_r$  of a central unit mass. Alternatively, this can also be seen as the probability distribution evolution equation of a system of two Brownian particles moving in their mutual gravitation field.

Equation (66) can be re-expressed as a Schrödinger equation (in imaginary time), thus involving a self-adjoint operator (see Appendix A). The large time behavior is dominated by the first eigenstate. Coming back to the notation of Eq. (66), we find that

$$(68) \quad \rho(r, t) \sim e^{-\lambda t} \psi(r),$$

where  $\psi$  satisfies the eigenequation

$$(69) \quad -\lambda \psi(r) = T \left( \psi'' + \frac{D-1}{r} \psi' \right) + \frac{1}{r^{D-1}} \psi',$$

and the same boundary condition as  $\rho$ , *i.e.*

$$(70) \quad T \psi'(1) + \psi(1) = 0.$$

The eigenvalue  $\lambda$  will also control the large time behavior of  $\rho_0$  and  $N_0$  as Eq. (52) and Eq. (68) both imply that

$$(71) \quad 1 - N_0(t) \approx \frac{\rho_0(t)}{\lambda} \sim e^{-\lambda t}.$$

We did not succeed in solving analytically the above eigenequation, and for a given temperature, this has to be solved numerically. However, in the limit of very small temperature, we can apply techniques reminiscent from semiclassical analysis in quantum mechanics ( $T \leftrightarrow \hbar$ ). We now assume  $T$  very small and define  $\phi$  such that

$$(72) \quad \psi(r) = e^{-\frac{\phi(r)}{T}}.$$

The function  $h = \phi'$  satisfies the following non-linear first order differential equation

$$(73) \quad T \left( h' + \frac{D-1}{r} h \right) + \frac{h}{r^{D-1}} - h^2 = \lambda T,$$

with the simple boundary condition

$$(74) \quad h(1) = 1.$$

In the limit  $T \rightarrow 0$ , the term proportional to  $T$  in the left-hand side of Eq. (73) can *a priori* be discarded leading to

$$(75) \quad h(r) = \frac{2\lambda T r^{D-1}}{1 + \sqrt{1 - 4\lambda T r^{2(D-1)}}}.$$

If  $4\lambda T < 1$ , the above expression is a valid perturbative solution also at  $r = 1$ , but cannot satisfy the constraint  $h(1) = 1$ . Hence, we conclude that in the limit of small temperature  $4\lambda T \geq 1$ , so that the above expression is only valid for  $r$  not too close to  $r = 1$ . The above argument also suggests that  $\lambda T$  is of order unity and we write

$$(76) \quad \lambda T = \frac{1}{4} + \mu^2.$$

To understand how the boundary condition Eq. (74) can be in fact satisfied, one has to come back to Eq. (73), which for  $r = 1$ , shows that  $h'(1) \sim \lambda \sim T^{-1} \gg 1$ . This implies that the term  $Th'$  cannot be neglected near  $r = 1$ , and that  $h$  varies in a noticeable way on a length scale from 1 of order  $T$ .

This suggests to define

$$(77) \quad z(x) = h(1 - Tx)$$

which satisfies (at order 0 in  $T$ )

$$(78) \quad -z' + z - z^2 = \frac{1}{4} + \mu^2,$$

and  $z(0) = 1$ . This equation has the unique solution

$$(79) \quad z(x) = \frac{1}{2} + \mu \frac{1 - 2\mu \tan(\mu x)}{2\mu + \tan(\mu x)}.$$

For large  $x$ , this function only has a sensible behavior for  $\mu = 0$ , which shows that

$$(80) \quad \lim_{T \rightarrow 0} \lambda T = \frac{1}{4},$$

and that Eq. (75) is in fact valid for  $1 - r \gg (4\lambda T - 1) \rightarrow 0$ . To leading order, we find

$$(81) \quad h(1 - Tx) \approx z_0(x) = \frac{1}{2} + \frac{1}{2+x}.$$

Equations (75) and (81), show that  $h(x)$  goes rapidly from 1 to 1/2 in a small region close to  $r = 1$  where  $h$  varies on the scale  $T$ . One can even compute the next correction to  $\lambda T$  by including the next term of order  $T$  in the equation for  $z$ . Writing

$$(82) \quad z(x) = z_0(x) + T^{1/3} z_1(x T^{1/3}),$$

we find

$$(83) \quad z_1' + \frac{2}{u} z_1 + z_1^2 - \frac{D-1}{2} u = -\frac{\mu^2}{T^{2/3}} = -c_D, \quad u = T^{1/3} x.$$

This is again an eigenvalue problem which selects a unique constant  $c_D$ , that we could only solve numerically. Still, this leads to the non trivial result

$$(84) \quad \lambda = \frac{1}{4T} + \frac{c_D}{T^{1/3}} + \dots \quad (T \rightarrow 0).$$

We now solve the eigenvalue problem (69) (70) in the limit of large temperatures  $T \rightarrow +\infty$  (see also Appendix A). We again perform the change of variables (72) and rewrite Eq. (73) in the form

$$(85) \quad h' + \frac{D-1}{r}h = \lambda - \frac{1}{T} \left( \frac{h}{r^{D-1}} - h^2 \right).$$

Then, we expand the solutions of this equation in terms of the small parameter  $1/T \ll 1$ . We write  $h = h_0 + \frac{1}{T}h_1 + \frac{1}{T^2}h_2 + \dots$  and  $\lambda = \lambda_0 + \frac{1}{T}\lambda_1 + \frac{1}{T^2}\lambda_2 + \dots$ . To zeroth order, we have

$$(86) \quad h'_0 + \frac{D-1}{r}h_0 = \lambda_0.$$

The solution of this equation is  $h_0 = \lambda_0 r/D$ . Using the boundary condition  $h_0(1) = 1$ , we obtain

$$(87) \quad \lambda_0 = D, \quad h_0 = r,$$

and  $h_n(1) = 0$  for  $n > 0$ . To first order, we get

$$(88) \quad h'_1 + \frac{D-1}{r}h_1 = \lambda_1 - \frac{h_0}{r^{D-1}} + h_0^2.$$

Integrating this first order differential equation and using the boundary condition  $h_1(1) = 0$ , we obtain

$$(89) \quad h_1 = \frac{D}{2(D+2)}r - \frac{1}{2}r^{3-D} + \frac{r^3}{D+2},$$

with

$$(90) \quad \lambda_1 = \frac{D^2}{2(D+2)}.$$

Hence, the large temperature behavior of the eigenvalue is

$$(91) \quad \lambda = D + \frac{D^2}{2(D+2)} \frac{1}{T} + \dots \quad (T \rightarrow +\infty).$$

This expansion can be easily carried out to higher orders but the coefficients are more and more complicated. Restricting ourselves to  $D = 3$ , we get  $\lambda = 3 + \frac{9}{10} \frac{1}{T} - \frac{477}{700} \frac{1}{T^2} + O(T^{-3})$ .

## 5 Numerical simulations in the canonical ensemble

In this section, we illustrate the analytical results obtained in the previous section in the case of  $D = 3$ . Except when specified otherwise, our simulations have been performed at  $T = 1/5 < T_c \approx 0.397 \dots$ , for which we have obtained  $t_{coll} \approx 0.44408 \dots$

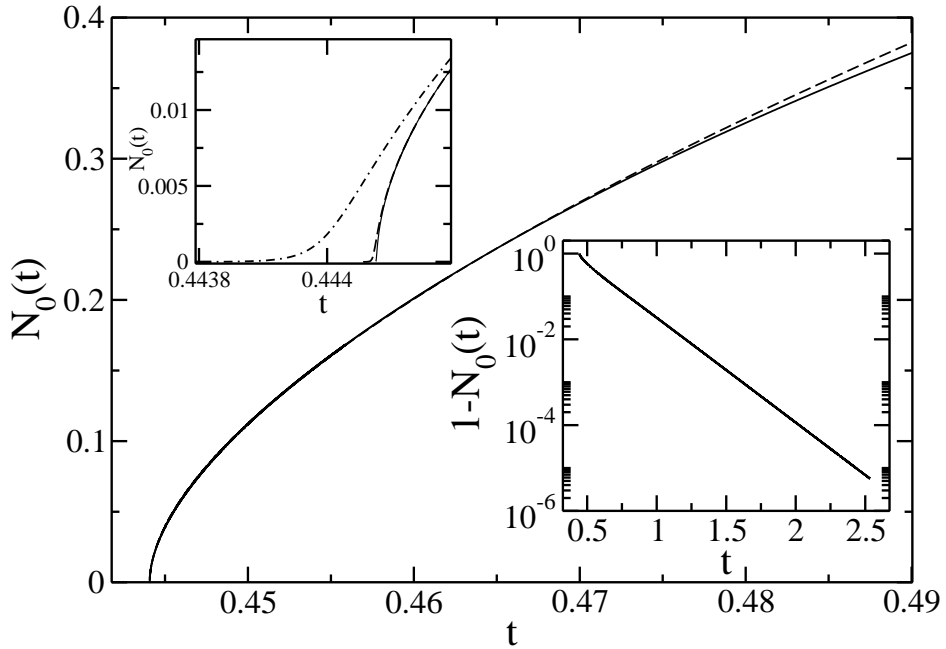


Figure 1: We plot  $N_0(t)$  for small times (full line). This is compared to  $N_0(t)^{\text{Theory}} \times [1 + a(t - t_{\text{coll}})^b]$  (dashed line), where  $N_0(t)^{\text{Theory}}$  is given by Eq. (64) with  $\mu = 8.38917147\dots$ , and  $a \approx 1.7$  and  $b \approx 0.33$  are fitting parameters. Note that the validity range of this fit goes well beyond the estimated  $t_*$  with  $t_* - t_{\text{coll}} \sim T^{D/2} \sim 0.09$ . The bottom insert illustrates the exponential decay of  $1 - N_0(t) \sim e^{-\lambda t}$ . The best fit for  $\lambda$  leads to  $\lambda \approx 5.6362$  to be compared to the eigenvalue computed by means of Eq. (69),  $\lambda = 5.6361253\dots$ . Finally, the top inset illustrates the sensitivity of  $N_0(t)$  to the space discretization, which introduces an effective cut-off (a factor 4 between each of the 3 curves). Note the small time scale. Even the curve corresponding to the coarsest discretization becomes indistinguishable from the others for  $t > 0.448$ .

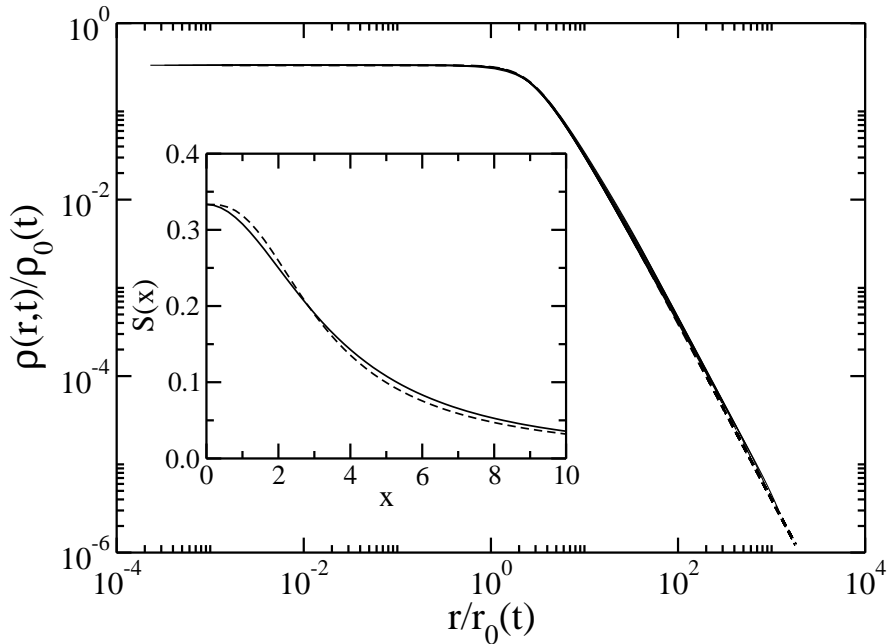


Figure 2: In the post-collapse regime, we plot  $\rho(r,t)/\rho_0(t)$  as a function of the scaling variable  $x = r/r_0(t)$ . A good data collapse is obtained for central residual densities in the range  $10^3 \sim 10^6$ . This is compared to the numerical scaling function computed from Eq. (62) (dashed line). The insert shows the comparison between this post-collapse scaling function (dashed line) and the scaling function below  $t_{coll}$  which has been rescaled to have the same value at  $x = 0$ , preserving the asymptotics:  $S(x) = (3 + x^2/4)^{-1}$  (see Eq. (19); full line). Note that the post-collapse scaling function is flatter near  $x = 0$ , as  $S(x) - 1/3 \sim x^3$  (in  $D = 3$ ) above  $t_{coll}$  instead of  $S(x) - 1/3 \sim x^2$ , below  $t_{coll}$ .

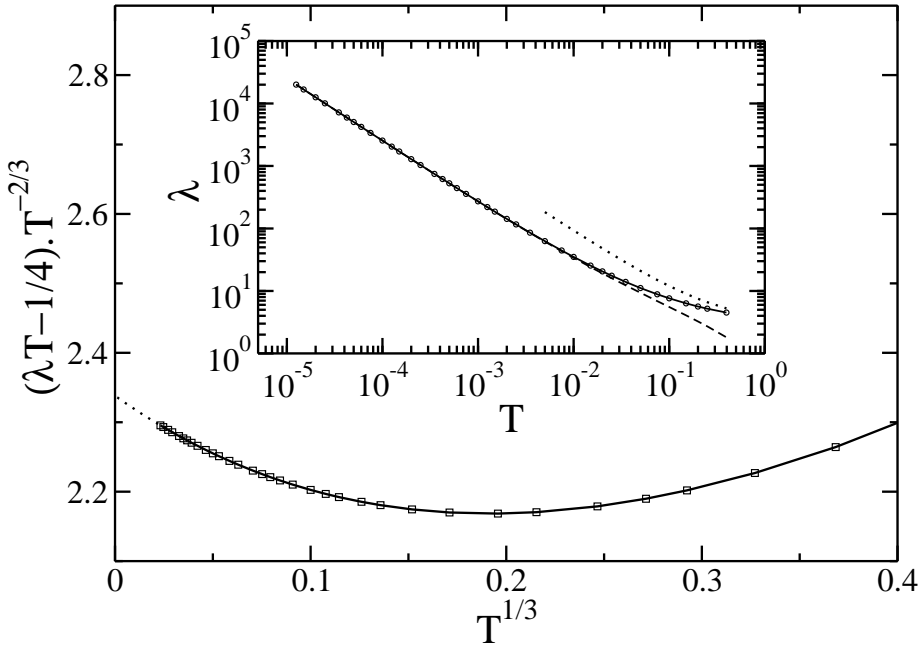


Figure 3: The main plot represents  $(\lambda T - \frac{1}{4}) T^{-2/3}$  as a function of  $T^{1/3}$  (line and squares), which should converge to  $c_{D=3} = 2.33810741\dots$  for  $T \rightarrow 0$  according to Eq. (84). We find a perfect agreement with this value using a quadratic fit (dotted line). Furthermore, this fit shows that the slope at  $T = 0$  is in fact equal to  $-2 \pm 2.10^{-4}$ , suggesting that the next term to the expansion of Eq. (84) is  $\lambda = \frac{1}{4T} + \frac{c_3}{T^{1/3}} - 2 + \dots$ , in  $D = 3$ . In the insert, we plot  $\lambda$  as a function of  $T$  up to  $T \approx T_c \approx 0.4$ . The small temperature analytical result of Eq. (84) is in very good agreement with the numerical data up to  $T \sim 0.03$ , whereas the large  $T$  estimate  $\lambda(T) = 3 + \frac{9}{10}T^{-1} + \dots$  is only qualitatively correct in this range of physical temperatures  $T \leq T_c$ .

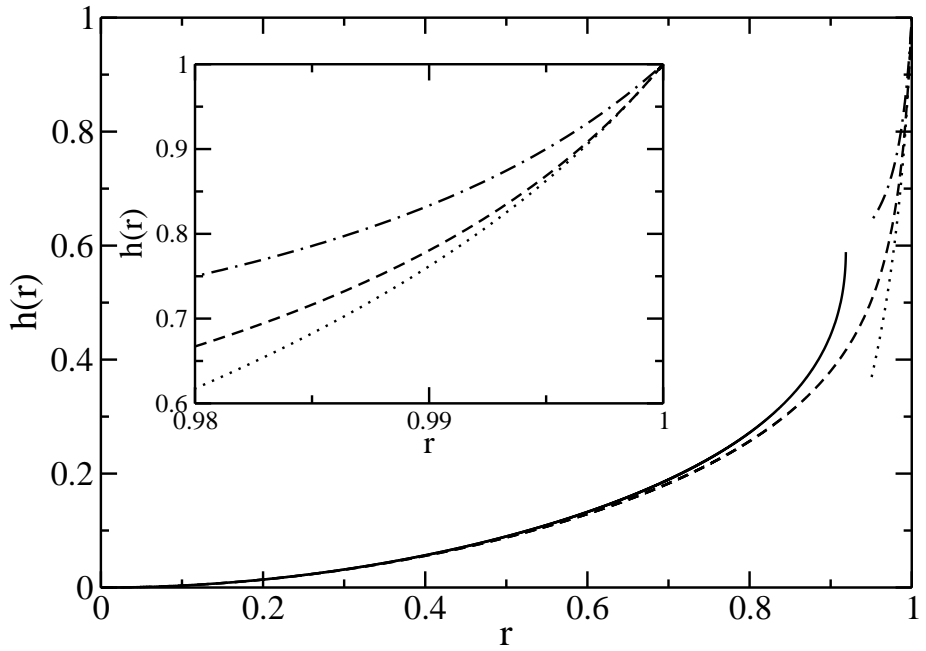


Figure 4: For  $T = 0.01$  ( $\lambda = 35.074198\dots$ ,  $\mu = 0.31739877\dots$ ), we plot  $h(r)$  computed numerically from Eq. (73) (dashed line), and the theoretical expression of Eq. (75), which is valid for  $1 - r \gg \mu^2 \sim T^{2/3}$  (full line). We also plot the theoretical expression of  $z_0$  (dashed-dot line; see Eq. (81)) and the next order perturbation result (dot line; see Eq. (82)), which are valid in the region  $1 - r \ll \mu^2 \sim T^{2/3}$ . The insert is a blow up of the region close to 1. Note how  $h(r)$  varies by a quantity of order unity as  $r$  varies by a quantity of order  $T = 0.01$ . We have chosen a not too small value for  $T$  in order to be able to visualize the two scale regimes on a single figure. Both approximations shown in the insert are getting better as  $T$  decreases.

In order to perform our simulations, we have used a Runge-Kutta algorithm with adaptive step in space and time. We call  $dr$  the spatial discretization near  $r = 0$  (which we need to take very small as the density profile becomes singular at  $r = 0$ ). An important numerical problem arises in the numerical integration of Eq. (52), which is crucial in obtaining non zero values for  $N_0(t)$ . As this equation is a first order differential equation with initial condition  $N_0(0) = 0$ , any naive integration scheme should lead to a strictly vanishing value for  $N_0(t)$  for all time, and any  $dr$ . Still, when performing this naive numerical integration, we see that crossing  $t_{coll}$  generates increasing values for  $M(dr, t)$ , although keeping  $M(0, t) = N_0(t) = 0$  ultimately makes the numerical integration unstable. In order to bypass this problem, we have decided to introduce a numerical scheme were Eq. (52) is replaced by

$$(92) \quad \frac{dN_0}{dt} = \rho_0^{fit} N_0^{fit}.$$

$N_0^{fit}$  and  $\rho_0^{fit}$  are extracted from a fit of  $M(r, t)$  to the functional form (we are in  $D = 3$ )

$$(93) \quad M(r, t) \approx N_0^{fit}(t) + \frac{\rho_0^{fit}(t)}{3} r^3 + a_5(t) r^5 + a_6(t) r^6,$$

in a region of a few  $dr$ , excluding of course  $r = 0$ . This functional form is fully compatible with the expected expansion for  $M(r, t)$ , both below ( $a_6 = 0$ ) and above ( $a_5 = 0$ )  $t_{coll}$ . We find that this numerical scheme allows us to cross smoothly the singularity at  $t_{coll}$ . An effective cut-off is introduced which effectively depends on  $dr$ , and we have checked that the result presented in this section are extremely close to the ones that would be obtained in the ideal limit  $dr \rightarrow 0$ . This is illustrated on Fig. 1, where the smoothing effect of our algorithm is shown to act on a very small time region after  $t_{coll}$ . Even more surprisingly, we find that for sufficiently large times (actually very small compared to any physical time scales), our results are essentially independent of  $dr$ , even for unreasonably large values of  $dr$ . We are thus confident that we have successfully crossed the collapse singularity.

In Fig. 1, we plot  $N_0(t)$  for small time which compares well with the universal form of Eq. (64), where  $\mu = 8.38917147\dots$  has been determined so as to ensure the proper behavior of  $S(x)$  for large  $x$  (see Sec. 4.1). We also illustrate the exponential decay of  $1 - N_0(t)$ , with a rate in perfect agreement with the value of  $\lambda$  extracted from solving numerically the eigenvalue problem of Eq. (69). Finally, we show the effect of the numerical spatial discretization  $dr$  near  $r = 0$ . Satisfactorily enough, the value of  $N_0(t)$  is sensitive to the choice of  $dr$  only for very small times after the collapse, and we were able to easily reach small enough  $dr$ , in order to faithfully reproduce the post-collapse singularity. In Fig. 2, we convincingly illustrate the post-collapse scaling, and compare the post-collapse scaling function to that obtained analytically below  $t_{coll}$  (pre-collapse). In Fig. 3, we confirm the validity of our perturbative expansion for  $\lambda$ , in the limit of small temperature. We compare the value of  $c_D$  extracted from directly solving the full eigenvalue problem to that obtained from Eq. (83), finding a perfect agreement. Finally, in Fig. 4, we compare the numerical value obtained for  $h(r)$  to the different analytical estimates given in the preceding section, for  $T = 0.01$ . The two important regions  $1 - r \ll \mu^2 \sim T^{2/3}$  and  $1 - r \gg \mu^2 \sim T^{2/3}$  can be clearly identified.

## 6 Post-collapse in the microcanonical ensemble

So far, we have only addressed the post-collapse dynamics in the canonical ensemble. In the microcanonical ensemble, the dynamical equation have to be supplemented with the strict energy conservation condition (see Eq. (7)), which fixes the global temperature  $T(t)$ . For this

model, it was shown in [1, 2, 3] that below a certain energy (Antonov energy), the system collapses with an apparent scaling associated with  $\alpha_{max} \approx 2.2$  for intermediate times (when the temperature still increases in a noticeable way) before entering a scaling regime with  $\alpha = 2$ , identical to that obtained in the canonical ensemble. In the limit  $t \rightarrow t_{coll}$ , the temperature and the potential energy both seem to converge to a finite value preserving a constant energy. This section addresses the  $t > t_{coll}$  time period.

Assuming a spherical mass density, and after integration by parts, the potential energy  $W$  can be rewritten in the form ( $D > 2$ )

$$(94) \quad W(t) = -\frac{1}{2} \int_0^1 \frac{M^2(r, t)}{r^{D-1}} dr - \frac{1}{2(D-2)}.$$

We see immediately that as  $D - 1 > 1$ , the occurrence of a finite mass  $N_0(t) \neq 0$  concentrated at  $r = 0$  implies an infinite potential energy, hence an infinite temperature. We thus anticipate that the post-collapse dynamics in the microcanonical ensemble is probably an ill-defined problem. In this extreme regime, let us try to consider the possible flaws of this model in order to describe a consistent dynamics of a reasonable physical self-gravitating system. First, our assumption of uniform temperature is certainly not realistic in a system displaying huge density contrast, and some alternative approaches are needed to incorporate a spatially dependent temperature. This point is certainly crucial and will be addressed in a future work [21]. Furthermore, in this regime, a careful physical analysis predicts that this system of self-gravitating individual particles should lead to the formation of binaries which is probably beyond the description ability of our essentially mean-field approach. In other words, the system may become intrinsically heterogeneous, which probably cannot be captured by our continuous model. Finally, we can think of other physical effects (degeneracy effects of quantum or dynamical origin, finite particle size effects,...) preventing the system from reaching arbitrarily large densities. One way to describe such effects consists in introducing a spatial cut-off  $h$  or a density cut-off of order  $h^{-D}$ . In such a system, the dynamics first follows the pre-collapse dynamics until the maximum density is approached. Then, the system will ultimately reach a maximum entropy state that we propose to characterize in a simple manner, as in [22, 19].

We propose to describe the final state as a “core-halo” structure, which for simplicity we modelize as a core of radius  $h \ll 1$  and constant density

$$(95) \quad \rho_{core} = \frac{DN_0}{S_D h^D},$$

which mimics a regularized central Dirac peak containing a mass  $N_0$ . In the region  $h < r \leq 1$  stands the halo of constant density

$$(96) \quad \rho_{halo} = \frac{D(1 - N_0)}{S_D(1 - h^D)},$$

containing the rest of the mass. As  $h$  is small, we can compute the potential (or total) energy and the entropy only including the relevant leading terms. We find

$$(97) \quad E = \frac{D}{2}T - \frac{D}{D^2 - 4} \left[ \frac{N_0^2}{h^{D-2}} + 1 + \frac{D-2}{2}N_0 - \frac{D}{2}N_0^2 \right] + O(h^2),$$

where the first term is the kinetic energy, whereas the entropy (up to irrelevant constants) reads

$$(98) \quad S = \frac{D}{2} \ln T - N_0 \ln \left( \frac{N_0}{h^D} \right) - (1 - N_0) \ln(1 - N_0) + O(h^D).$$

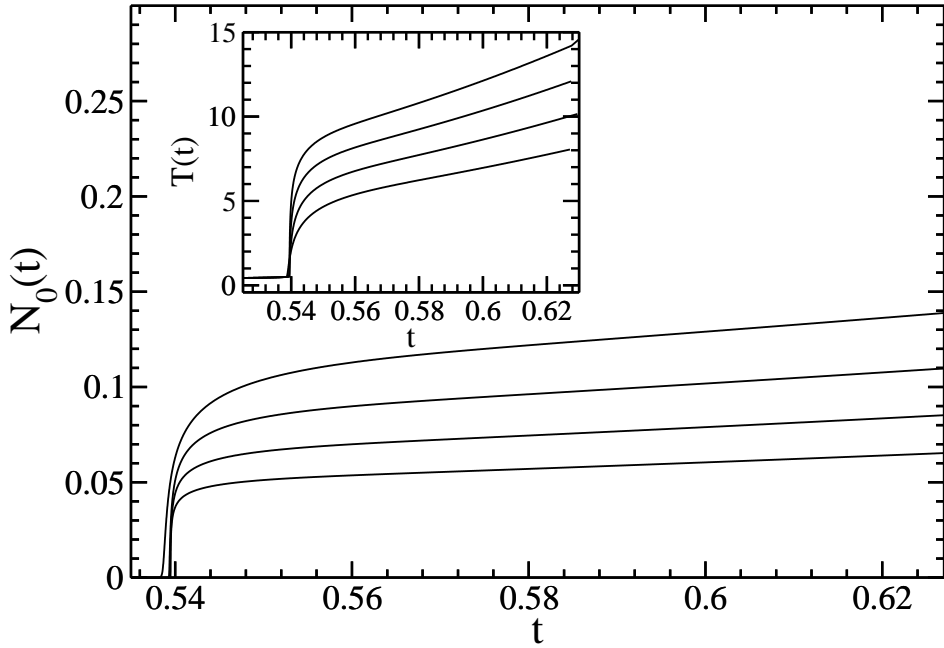


Figure 5: For  $E = -0.45 < E_c \approx -0.335$ , we plot  $N_0(t)$ , for different values of  $h$  decreasing by a factor 2 for each curve from the top one to the bottom one. It is clear that  $N_0(t)$  decreases as  $h$  decreases. The insert shows the corresponding temperature plots. The temperature  $T(t)$  increases as  $h$  decreases. Note that in the pre-collapse regime, the temperature essentially does not depend on  $h$ . For the situation considered, it starts from  $T(0) = 0.1$  and culminates at  $T(t_{coll}) \approx 0.5$ .

For a given small value of  $h$ ,  $S$  has a local maximum at  $N_0 = 0$  provided that  $E > E_c(h)$ , with  $\lim_{h \rightarrow 0} E_c(h) = -\frac{D}{D^2-4}$ . Below  $E_c$ , the sole entropy maximum resides at  $N_0$  satisfying the following implicit equation (again in the limit of small  $h$ )

$$(99) \quad N_0 = \frac{D}{\ln\left(\frac{N_0}{h^D}\right)} \sim -\frac{1}{\ln h},$$

where the given asymptotics is quantitatively correct only for extremely small values of  $h$ . Hence, we find that the mass included in the core slowly *decreases* with the core size  $h$  [19]. Meanwhile, the temperature diverges as

$$(100) \quad T \sim -\frac{2}{D}W \sim \frac{2}{D^2-4} \frac{1}{h^{D-2} \ln^2 h}.$$

and leads rapidly and efficiently to a uniform halo.

In order to relate this result to our actual system, we perform microcanonical post-collapse simulations using the same regularization scheme as in the canonical case in order to describe the evolution of  $N_0(t)$ . In addition to this, we also need to regularize the potential energy which is strictly infinite (as well as  $T$ ) when  $N_0 \neq 0$ . Consistently with the previous discussion, we introduce a numerical cut-off  $h$  by defining

$$(101) \quad W(t) = -\frac{1}{2} \int_h^1 \frac{M^2(r, t)}{r^{D-1}} dr - \frac{1}{2(D-2)}.$$

In Fig. 5, we plot  $N_0(t)$  and  $T(t)$  for different values of the cut-off  $h$ . Contrary to the canonical case, the post-collapse dynamics is strongly  $h$  dependent. We see that in conformity with

our result of Eq. (99), the central mass  $N_0$  clearly decreases as  $h \rightarrow 0$ . Therefore, in the microcanonical case, the physical picture is that when the collapse time  $t_{coll}$  is reached, the temperature increases rapidly, which leads to the rapid homogenization of the system except for a dense and small core, whose mass  $N_0 \sim \ln^{-1} T$  is a decreasing function of the maximum temperature reached. This central structure with weak mass and huge binding energy is similar to a “binary star” structure in stellar dynamics. Binary formation is the physical process that arrests core collapse in globular clusters [23]. This is also the end point of our simple microcanonical Brownian model.

## 7 Conclusion

In this paper, we have investigated the post-collapse dynamics of a gas of self-gravitating Brownian particles in canonical and microcanonical ensembles. At the collapse time  $t_{coll}$ , the system develops a singular density profile scaling as  $\rho \sim r^{-2}$ . However, the “central singularity contains no mass”, the temperature does not diverge, and the entropy and free energy are finite [1, 2, 3]. Since this profile is not a maximum entropy (resp. free energy) state nor a stationary solution of the Smoluchowski-Poisson system, the collapse continues after  $t_{coll}$ .

In the canonical ensemble, mass accretes progressively at the center of the system and a Dirac peak forms by swallowing the surrounding particles. Eventually, the Dirac peak contains all the mass. This structure has an infinite free energy  $J = S - \beta E$  simply because its binding energy is infinite. This is therefore the most probable structure in canonical ensemble [16, 18, 19]. In the microcanonical ensemble, the maximum entropy state (at fixed mass and energy) consists of a single binary embedded in a hot halo [15, 17, 2]. This is precisely what we see in our numerical simulations. The temperature increases dramatically above  $t_{coll}$  (resulting in an almost uniform halo) although the mass contained in the core is weak (but finite). We note the “spectacular” fact that almost all the gravitational energy resides in a binary-like core with negligible mass. A similar phenomenon is observed in stellar dynamics for globular clusters having experienced core collapse [20]. This shows that the microcanonical Smoluchowski-Poisson system shares some common properties with kinetic equations usually considered in stellar dynamics (Landau-Fokker-Planck equations), despite its greater simplicity. Clearly, a major drawback of our microcanonical model is to assume that the temperature uniformizes instantaneously, implying an infinite thermal conductivity. We shall relax this simplification in a future work [21]. To our knowledge, the present study is the first dynamical study showing the formation of Dirac peaks and binary-like structures for self-gravitating systems.

## A Brownian particle around a “black hole”

We consider the Brownian motion of a particle subject to the gravitational force  $-GM\mathbf{r}/r^3$  created by a central mass  $M$  (“black hole”). We assume that when the particle comes at  $r = 0$ , it is captured by the central mass. We denote by  $W(\mathbf{r}, t)$  the density probability of finding the particle in  $\mathbf{r}$  at time  $t$ . It is solution of the Fokker-Planck equation

$$(102) \quad \frac{\partial W}{\partial t} = \nabla \left( T \nabla W + W \frac{\mathbf{r}}{r^3} \right),$$

where we have set  $G = M = R = \xi = 1$ . Let  $W(r, t)$  denote a spherically symmetric solution of Eq. (102) satisfying the boundary conditions

$$(103) \quad T \frac{\partial W}{\partial r}(1, t) + W(1, t) = 0,$$

$$(104) \quad W(r, 0) = \frac{\delta(r - r_0)}{4\pi r_0^2}.$$

We call

$$(105) \quad \mathbf{J} = - \left( T \nabla W + W \frac{\mathbf{r}}{r^3} \right),$$

the current of probability, i.e.  $\mathbf{J} dS \mathbf{n}$  gives the probability that the particle crosses an element of surface  $dS$  between  $t$  and  $t + dt$  ( $\mathbf{n}$  is a unit vector normal to the element of surface under consideration).

We introduce the probability  $p(r_0, t)dt$  that a particle located initially between  $r_0$  and  $r_0 + dr_0$  arrives for the first time at  $r = 0$  between  $t$  and  $t + dt$ . We have

$$(106) \quad p(r_0, t) = - \int_{R_\epsilon} \mathbf{J} \cdot d\mathbf{S} = 4\pi\epsilon^2 \left( T \frac{\partial W}{\partial r} + \frac{W}{r^2} \right)_\epsilon = 4\pi W(0, t),$$

where  $R_\epsilon$  is a ball of radius  $\epsilon \rightarrow 0$ . The total probability that the particle initially between  $r_0$  and  $r_0 + dr_0$  has reached the center of the system between 0 and  $t$  is thus

$$(107) \quad Q(r_0, t) = \int_0^t p(r_0, t') dt'.$$

Finally, we average  $Q(r_0, t)$  over an appropriate range of initial positions in order to get the expectation  $Q(t)$  that the particle has been captured at time  $t$ .

With the change of variables

$$(108) \quad W = \psi e^{\frac{1}{2Tr}},$$

we can transform the Fokker-Planck equation (102) into a Schrödinger equation (in imaginary time) of the form

$$(109) \quad \frac{\partial \psi}{\partial t} = T \Delta \psi - \frac{1}{4Tr^4} \psi.$$

A separation of the variables can be effected by the substitution

$$(110) \quad \psi = \phi(r) e^{-\lambda t}.$$

This transformation reduces the Schrödinger equation to a second order ordinary differential equation

$$(111) \quad \phi'' + \frac{2}{r}\phi' + \left(\frac{\lambda}{T} - \frac{1}{4T^2r^4}\right)\phi = 0,$$

with the boundary condition

$$(112) \quad \phi'(1) + \frac{1}{2T}\phi(1) = 0.$$

We note  $\lambda_n$  the eigenvalues and  $\phi_n$  the corresponding eigenfunctions. Since the Schrödinger operator  $H = \Delta - 1/4T^2r^4$  is Hermitian, the eigenfunctions form a complete set of orthogonal functions for the scalar product

$$(113) \quad \langle fg \rangle = \int_0^1 f(r)g(r)4\pi r^2 dr.$$

The system can be furthermore normalized, i.e.  $\langle \phi_n \phi_m \rangle = \delta_{nm}$ . Any function  $f(r)$  satisfying the boundary condition (112) can be expanded on this basis, as

$$(114) \quad f(r) = \sum_n \langle f \phi_n \rangle \phi_n.$$

In particular,

$$(115) \quad \frac{\delta(r - r_0)}{4\pi r_0^2} = \sum_n \phi_n(r_0) \phi_n(r).$$

The general solution of the problem (102) (103) can be expressed in the form

$$(116) \quad W(r, t) = \sum_n A_n e^{-\lambda_n t} e^{\frac{1}{2Tr}} \phi_n(r),$$

where the coefficients  $A_n$  are determined by the initial conditions (104), using the expansion (115) for the  $\delta$ -function. We get

$$(117) \quad W(r, t) = e^{\frac{1}{2T}(\frac{1}{r} - \frac{1}{r_0})} \sum_n e^{-\lambda_n t} \phi_n(r_0) \phi_n(r).$$

From this expression, we obtain

$$(118) \quad p(r_0, t) = 4\pi e^{-\frac{1}{2Tr_0}} \sum_n e^{-\lambda_n t} \phi_n(r_0) \lim_{r \rightarrow 0} \left[ \phi_n(r) e^{\frac{1}{2Tr}} \right].$$

Then, according to Eq. (107), we have

$$(119) \quad Q(r_0, t) = 4\pi e^{-\frac{1}{2Tr_0}} \sum_n \frac{1 - e^{-\lambda_n t}}{\lambda_n} \phi_n(r_0) \lim_{r \rightarrow 0} \left[ \phi_n(r) e^{\frac{1}{2Tr}} \right].$$

Finally, averaging over the initial conditions, the probability that the particle has been captured by the central mass at time  $t$  can be expressed as

$$(120) \quad Q(t) = \sum_n Q_n(t),$$

where

$$(121) \quad Q_n(t) = B_n(1 - e^{-\lambda_n t}),$$

and

$$(122) \quad B_n = 4\pi \frac{1}{\lambda_n} \overline{e^{-\frac{1}{2Tr_0}} \phi_n(r_0)} \lim_{r \rightarrow 0} \left[ \phi_n(r) e^{\frac{1}{2Tr}} \right].$$

This formally solves the problem. If we consider the large time limit, we just need to determine the first eigenvalue  $\lambda_0(T)$  of the quantum problem. This has been done analytically in Sec. 4.2 in the limits  $T \rightarrow 0$  and  $T \rightarrow +\infty$ .

Below, we consider again the high temperature regime where thermal fluctuations prevail over gravity but we do not restrict ourselves to the first eigenvalue. To leading order in the limit  $T \rightarrow +\infty$ , the Fokker-Planck equation (102) reduces to the pure diffusion equation

$$(123) \quad \frac{\partial W}{\partial t} = T \frac{1}{r^2} \frac{\partial}{\partial r} \left( r^2 \frac{\partial W}{\partial r} \right).$$

However, for consistency (see Sec. 4.2), it is necessary to keep the term of order  $1/T$  (arising from the gravitational force) in the boundary condition. Hence, we take

$$(124) \quad \frac{\partial W}{\partial r}(1, t) + \frac{1}{T} W(1, t) = 0.$$

The general solution of the diffusion equation (123) with the boundary conditions (124) and (104) can be expressed as

$$(125) \quad W(r, t) = \sum_n e^{-\lambda_n t} \phi_n(r_0) \phi_n(r),$$

where  $\phi$  is solution of

$$(126) \quad \phi'' + \frac{2}{r} \phi' + \frac{\lambda}{T} \phi = 0,$$

$$(127) \quad \phi'(1) + \frac{1}{T} \phi(1) = 0.$$

Setting  $\phi = \chi/r$ , Eqs. (126) and (127) become

$$(128) \quad \chi'' + \frac{\lambda}{T} \chi = 0,$$

$$(129) \quad \chi'(1) = \left( 1 - \frac{1}{T} \right) \chi(1).$$

Equation (128) is readily solved. The eigenvalues can be written  $\lambda_n = Tx_n^2(T)$ , where  $x_n(T)$  are the solutions of the implicit equation

$$(130) \quad \tan(x_n) = \frac{x_n}{1 - \frac{1}{2T}}.$$

The eigenfunctions are

$$(131) \quad \phi_n(r) = A_n \frac{\sin(x_n r)}{r}.$$

The general solution of the diffusion equation can thus be written

$$(132) \quad W(r, t) = \frac{1}{rr_0} \sum_{n=0}^{+\infty} e^{-Tx_n^2 t} A_n^2 \sin(x_n r) \sin(x_n r_0),$$

with

$$(133) \quad A_n^2 = \frac{x_n}{2\pi(x_n - \sin x_n \cos x_n)}.$$

If we consider the pure diffusion of a particle in a box, the boundary condition (127) reduces to  $\phi'(1) = 0$  and the  $x_n$  are solutions of the implicit equation

$$(134) \quad \tan(x_n) = x_n.$$

In particular,  $x_0 = 0$ . This implies that the probability  $W(r, t)$  converges for large times to a *uniform* profile  $W(r, +\infty) = 3/4\pi$  which is indeed solution of the diffusion equation in a box. If gravity is taken into account, its first order effect (in the limit  $T \rightarrow +\infty$ ) is to change the boundary condition to Eq. (127). It is *as if* we had a diffusion across the box [24, 9] although the true physical process is a capture by the central mass. The eigenvalues are now determined by Eq. (130). The  $x_{n>1}$  are hardly modified (to first order) with respect to the preceding problem but  $x_0$  is now different from zero. To first order, we find that  $x_0^2 = 3/T$  so that  $\lambda_0 = 3$  in agreement with the result of Sec. 4.2. We also note that  $A_0^2 = T/4\pi$  while  $A_{n>0}$  are independent on  $T$  (to leading order) and given by Eqs. (133) and (134).

Using Eqs. (106) and (107), the probability that the particle has been captured by the central mass at time  $t$  is given by

$$(135) \quad Q(t) = \frac{4\pi}{T} \sum_{n=0}^{+\infty} \frac{1 - e^{-Tx_n^2 t}}{x_n} A_n^2 \frac{\overline{\sin(x_n r_0)}}{r_0}.$$

If we average over initial conditions with the weight  $3r_0^2$  (uniform distribution), we find to leading order in  $T^{-1}$  that

$$(136) \quad \frac{\overline{\sin(x_n r_0)}}{r_0} = 0, \quad \text{for } n > 0,$$

$$(137) \quad \frac{\overline{\sin(x_0 r_0)}}{r_0} = x_0.$$

Hence, the modes  $n > 0$  cancel out. Therefore, in the high temperature regime, the probability of capture is given by

$$(138) \quad Q(t) = 1 - e^{-3t},$$

for all times.

The case  $D = 2$  can be treated by a similar method. Instead of Eqs. (132) (133) and (130), we get

$$(139) \quad W(r, t) = \sum_{n=0}^{+\infty} e^{-Tx_n^2 t} A_n^2 J_0(x_n r) J_0(x_n r_0),$$

$$(140) \quad A_n^2 = \frac{1}{\pi [J_1^2(x_n) + J_0^2(x_n)]},$$

$$(141) \quad \frac{x_n J_1(x_n)}{J_0(x_n)} = \frac{1}{T},$$

where  $J_n$  is the Bessel function of order  $n$ . For the pure diffusion process,  $x_n = \alpha_{1n}$  are the zeros of  $J_1$ . If gravity is taken into account, then  $x_{n>1} \simeq \alpha_{1n}$  while  $x_0^2 = 2/T$  establishing  $\lambda_0 = 2$ . The probability that the particle has been captured by the central mass at time  $t$  is given by

$$(142) \quad Q(t) = \frac{2\pi}{T} \sum_{n=0}^{+\infty} \frac{1 - e^{-Tx_n^2 t}}{x_n^2} A_n^2 \overline{J_0(x_n r_0)}.$$

If we average over the initial conditions with a weight  $2r_0$  (uniform distribution), we get  $\overline{J_0(x_n r_0)} = 0$  if  $n > 0$  and  $\overline{J_0(x_0 r_0)} = 1$ . Therefore, in the high temperature regime, the probability of capture is given, for all times, by

$$(143) \quad Q(t) = 1 - e^{-2t}.$$

Finally, for  $D = 1$ , we obtain

$$(144) \quad W(r, t) = \sum_{n=0}^{+\infty} e^{-Tx_n^2 t} A_n^2 \cos(x_n r) \cos(x_n r_0),$$

$$(145) \quad A_n^2 = \frac{1}{[1 + \frac{\sin(2x_n)}{2x_n}]},$$

$$(146) \quad x_n \tan(x_n) = \frac{1}{T}.$$

For the pure diffusion process,  $x_n = n\pi$ . If gravity is taken into account, then  $x_{n>1} \simeq n\pi$  while  $x_0^2 = 1/T$  establishing  $\lambda_0 = 1$ . The probability that the particle has been captured by the central mass at time  $t$  is given by

$$(147) \quad Q(t) = \frac{2}{T} \sum_{n=0}^{+\infty} \frac{1 - e^{-Tx_n^2 t}}{x_n^2} A_n^2 \overline{\cos(x_n r_0)}.$$

If we average over the initial conditions with a weight 1 (uniform distribution), we get  $\overline{\cos(x_n r_0)} = 0$  if  $n > 0$  and  $\overline{\cos(x_0 r_0)} = 1$ . Therefore, in the high temperature regime, the probability of capture is given, for all times, by

$$(148) \quad Q(t) = 1 - e^{-t}.$$

## References

- [1] P.H. Chavanis, C. Rosier and C. Sire, Phys. Rev. E **66**, 036105 (2002).
- [2] C. Sire and P.H. Chavanis, Phys. Rev. E **66**, 046133 (2002).
- [3] P.H. Chavanis and C. Sire, to appear in Phys. Rev. E [cond-mat/0303088].
- [4] M.V. Penston, Mon. Not. R. astr. Soc. **144**, 425 (1969).
- [5] R.B. Larson, Mon. Not. R. astr. Soc. **147**, 323 (1970).
- [6] H. Cohn, Astrophys. J. **242**, 765 (1980).
- [7] D. Lynden-Bell and P.P. Eggleton, Mon. Not. R. astr. Soc. **191**, 483 (1980).
- [8] C. Lancellotti and M. Kiessling, Astrophys. J. **549**, L93 (2001).
- [9] P.H. Chavanis, Astron. Astrophys. **356**, 1089 (2000)
- [10] P.H. Chavanis, J. Sommeria and R. Robert, Astrophys. J. **471**, 385 (1996).
- [11] C. Rosier, C. R. Acad. Sci., Ser. I: Math. **332**, 903 (2001).
- [12] P. Biler and T. Nadzieja, Rep. Math. Phys., in press (2003)
- [13] J.D. Murray, *Mathematical Biology* (Springer, 1991).
- [14] I.A. Guerra, M.A. Peletier and J. Williams, preprint.
- [15] V.A. Antonov, Vest. Leningr. Gos. Univ. **7**, 135 (1962).
- [16] M. Kiessling, J. Stat. Phys. **55**, 203 (1989).
- [17] T. Padmanabhan, Phys. Rep. **188**, 285 (1990).
- [18] P.H. Chavanis, Astron. Astrophys. **381**, 340 (2002).
- [19] P.H. Chavanis, Phys. Rev. E, **65**, 056123 (2002).
- [20] J. Binney and S. Tremaine, *Galactic Dynamics* (Princeton Series in Astrophysics, 1987).
- [21] C. Sire and P.H. Chavanis, in preparation.
- [22] P.H. Chavanis and J. Sommeria, Mon. Not. R. astr. Soc. **296**, 569 (1998).
- [23] M. Hénon, Ann. Astrophys. **5**, 369 (1961).
- [24] S. Chandrasekhar, Astrophys. J. **97**, 263 (1943).